# Measurement of the Triple-Scattering Parameter $A$ in Proton-Proton and Proton-Carbon Scattering at 139 MeV*

STANLEY HEE AND E. H. THORNDIKE†
*Cyclotron Laboratory, Harvard University, Cambridge, Massachusetts*
(Received 3 June 1963)

The proton-proton triple-scattering parameter $A$ has been measured at a laboratory energy of 139 MeV over a range of scattering angles $\theta_2$. The following values were obtained: $\theta_2$(lab)=15°, $-0.368\pm0.032$; 20°, $-0.344\pm0.031$; 25°, $-0.311\pm0.035$; 30°, $-0.231\pm0.046$; 35°, $-0.187\pm0.056$; 40°, $-0.099\pm0.079$. The parameter was also determined for $p$-carbon scattering at $\theta_2$(lab)=15° with a laboratory scattering energy of $138\frac{1}{2}$ MeV. The value obtained was $-0.531\pm0.048$. The measurements are subject to a systematic error, which could shift all values of $A$ up or down together by perhaps 4%. In the errors listed above, this systematic error has been combined quadratically with the other errors, which are of a nonsystematic nature.

## INTRODUCTION

THIS experiment continues the program of measuring $p$-$p$ scattering parameters near 140 MeV. The cross section,[1] polarization,[1] depolarization parameter $D$,[2] and rotation $R$,[3] have already been measured. This article describes a measurement of the triple scattering parameter $A$ for $p$-$p$ scattering at 139 MeV over the range of laboratory scattering angles, 15° to 40°. Also included is a measurement of $A$ for $p$-carbon scattering at $138\frac{1}{2}$ MeV at a scattering angle of 15° lab. The parameter $A$, as defined by Wolfenstein,[4] relates the incident polarization along the direction of motion to the component of polarization after scattering transverse to the direction of motion and in the plane of scattering.

The experimental arrangement for the $p$-$p$ measurement is shown in Fig. 1. A vertically polarized proton beam passes through a solenoid magnet ($R$). The polarization precesses 90° about the direction of motion, so that on leaving the solenoid the beam has a polarization in the horizontal plane and perpendicular to the direction of motion. The beam then passes through a door-frame-type sector electromagnet ($M$) which bends the beam through an angle of approximately 44°. This produces a beam with polarization $P_1$ parallel to the direction of motion. This longitudinally polarized beam strikes a liquid-hydrogen target (2). Particles scattered through an angle $\theta_2$ in the horizontal plane, as defined by counters $A$, $B$, strike the analyzing scatterer (3). Some are here scattered through an angle $\theta_3$ in the vertical plane containing the line from the hydrogen target to the analyzing scatterer. Counter telescopes $CD$ and $EF$ are set at the angle $\theta_3$ to detect these particles. The angle $\theta_3$ of the telescopes can be reversed in sign, and we denote the up and down positions by $U$ and $D$, respectively. The direction of the current through the solenoid, and, hence, the sign of the longitudinal polarization $P_1$ can also be reversed. The two possibilities are denoted by $N$ and $R$ (for normal and reversed).

Let $I(k,m)$ be the rate of fourfold coincidences ($ABCD$ or $ABEF$) for counter telescope position $k$ and solenoid current direction $m$, where $k$ is either $U$ or $D$, and $m$ is either $N$ or $R$. If we write

$$e_{3s}=\frac{I(D,N)+I(U,R)-I(U,N)-I(D,R)}{I(D,N)+I(U,R)+I(U,N)+I(D,R)}, \quad (1)$$

then $A$ is defined by the equation

$$e_{3s}=-AP_1P_3. \quad (2)$$

The product of incident polarization and analyzing power, $P_1P_3$, is measured following the same convention as to solenoid current direction and telescope position. For its measurement, however, the sector magnet ($M$) must be removed.

The apparatus and techniques used in this experiment are, with a few exceptions, identical to those used

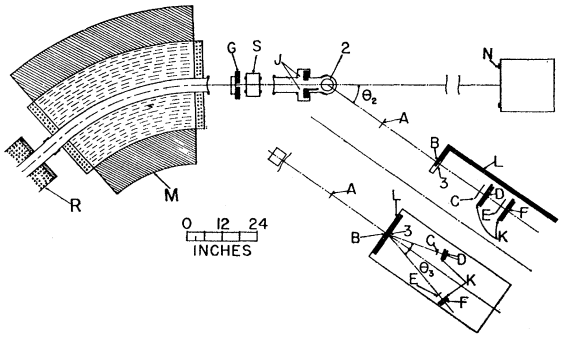


FIG. 1. Scale drawing of the experimental arrangement showing: (2) hydrogen target, (3) analyzing scatterer, ($A$–$F$) scintillation counters, ($G$) main defining slits, ($J$) antiscattering slits, ($K$) copper absorbers, ($L$) iron shielding, ($M$) sector magnet, ($N$) Faraday cup, ($R$) solenoid magnet, ($S$) ion chamber. The inset (lower right) shows an elevation of the analyzing scattering.

* Supported by the joint program of the Office of Naval Research and the U. S. Atomic Energy Commission.
† Present address: Department of Physics, University of Rochester, Rochester, New York.
[1] J. N. Palmieri, A. M. Cormack, N. F. Ramsey, and Richard Wilson, Ann. Phys. (N. Y.) **5**, 229 (1958).
[2] C. F. Hwang, T. R. Ophel, E. H. Thorndike, and Richard Wilson, Phys. Rev. **119**, 352 (1960).
[3] E. H. Thorndike, J. Lefrançois, and Richard Wilson, Phys. Rev. **120**, 1819 (1960).
[4] L. Wolfenstein, Ann. Rev. Nucl. Sci. **6**, 43 (1956).

for measuring $R$.[3] The differences between experiments are:

(1) The sector magnet ($M$) was used for measuring $A$, but not for measuring $R$.

(2) $P_1P_3$ was not measured during the $A$ experiments. Its values were inferred by an indirect method from the values measured during the $R$ experiment.

(3) During the $A$ measurement, the $\theta_3$ misalignments were greatly reduced by a deflecting field. This deflecting field was not used during the $R$ measurement.

(4) During the $R$ experiment, measurements were made for both senses of the scattering angle $\theta_2$; during the $A$ experiment, $\theta_2$ had only the sense shown in Fig. 1.

For matters not involving the four differences listed above, greater detail than is here given is found in Ref. 3.

## EXPERIMENTAL PROCEDURE

### Beam and Magnets

The beam used was the polarized proton beam of the Harvard synchrocyclotron.[5] After passing through the magnet system it is defined by slits ($G$), $1\frac{3}{8}$-in. wide by 2-in. high. The mean energy was 143 MeV. The polarization, believed to be the same as in the $R$ experiment,[3] is now estimated at 61%.

As the beam passes through the solenoid, its polarization precesses about the magnetic field.[6] The solenoid field was kept within 1% of the value which rotates the polarization of a $144\frac{1}{2}$-MeV beam through 90°, and a 143-MeV beam through $90\frac{1}{2}$°.

Upon leaving the solenoid, the beam immediately passes through the sector magnet which is designed to bend the beam through an angle near 44° along a mean radius of 56 in. The current through the coils of the sector magnet was regulated to 0.3%. The beam emerging from the sector magnet no longer has its polarization vector perpendicular to the direction of motion. Rather, the polarization has been rotated relative to the beam direction, through an angle $\chi$ which is nonzero because of the anomalous part of the proton magnetic moment.[6] Consequently, the beam has acquired a longitudinal component of polarization equal to $\pm P_1 \sin\chi$. (The upper sign refers to solenoid $N$, the lower to solenoid $R$.) From the equations in Ref. 6, the angle of bend for a 143-MeV proton beam should be 43.6° for $\chi=90°$.

In addition to producing the desired longitudinal polarization, the solenoid and sector magnets affect the beam in other ways. The fringing field of the cyclotron-magnet energy analyzes the proton beam. With the solenoid off, the beam emerging from the solenoid beam pipe has a sharp high-energy edge on the south side; the beam fills the pipe to the north of this edge. Figure 2(a) shows how this would appear on x-ray film. The horizontal energy dispersion at this point is 5 MeV/in. The sector magnet bends in the opposite direction from the cyclotron magnet, and to a large extent, cancels the energy dispersion. At the exit of the sector magnet, the image of the round solenoid beam pipe can be seen on the north [see Fig. 2(b)]. The width of the beam is less than at the solenoid exit. Some of the low-energy protons have been bent across the pipe, and now appear to the south of the high-energy edge. A typical positioning of the defining slits is given by the rectangle.

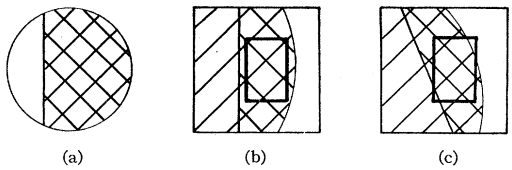


FIG. 2. Sketches of the polarized proton beam with relation to the beam pipes and main defining slits.

When the solenoid is turned on, the image of the beam as a whole is rotated by approximately 16°. The edges of the beam may now cut across the slit openings as indicated in Fig. 2(c). This nonuniformity of the beam in the vertical direction produces an apparent shift in the $\theta_3=0°$ position from solenoid $N$ to solenoid $R$. To compensate for this effect, a set of dipole windings was installed on one of the quadrupole focussing magnets, just before the entrance to the solenoid, so as to deflect the beam, as a whole, up or down. The current through the dipole windings was reversed with the solenoid current, thereby keeping the normal minus reverse misalignments of both counters below 0.04° for all $e_{3s}$ measurements.

The rotation of the beam image by the solenoid introduces a vertical energy dispersion. At the exit of the solenoid, this dispersion is $1\frac{1}{4}$ MeV/in., with the energy highest at the bottom when the solenoid is normal, and at the top when the solenoid is reversed. This dispersion necessitated a correction to the $R$ measurements. However, the sector magnet largely cancels the dispersion; at the defining slits, the solenoid-dependent vertical energy dispersion was measured to be $0.13\pm0.50$ MeV/in.

### Alignment

The alignment procedure was in all essential aspects the same as that used in the $R$ experiment.[3] The "slope method" was used to calculate the misalignment as given by

$$\Delta\theta_s(\theta_i)=\frac{2[A(\theta_i,U)-A(\theta_i,D)]}{A(\theta_{i-1},U)+A(\theta_{i-1},D)-A(\theta_{i+1},U)-A(\theta_{i+1},D)}, \tag{3}$$

or by

$$\Delta\theta_s'(\theta_i)=\frac{\pm[A(\theta_i,U)-A(\theta_i,D)]}{A(\theta_i,U)+A(\theta_i,D)-A(\theta_{i\pm1},U)-A(\theta_{i\pm1},D)}, \tag{4}$$

[5] G. Calame, P. Cooper, S. Engelsberg, G. Gerstein, A. Koehler, A. Kuckes, J. Meadows, K. Strauch, and R. Wilson, Nucl. Instr. 1, 169 (1956).

[6] H. Mendlowitz and K. M. Case, Phys. Rev. 97, 33 (1955).

where $A(\theta_i)$ is the counting rate at analyzing angle $\theta_i$. The angles used were 2°, 3°, 4°, 5° for the *EF* telescope and 3°, 4°, 5°, 6° for the *CD* telescope. Wherever the full first moment $\Delta\theta_0$ (as defined in Ref. 3) was not measured, it was approximated by an average of $\Delta\theta_s$ and $\Delta\theta_s'$ over the four angles used in the measurement.

The only significant change in the alignment procedure was the use of the dipole windings. This resulted in a reduction in the normal minus reverse misalignment by a factor near 12.

The alignment correction was calculated using the $(1/\sigma)d\sigma/d\theta$ values of Ref. 3, interpolating where necessary. The errors were suitably expanded to take into account the uncertainties of the interpolation process. Because of the small absolute value of the measured misalignment, the correction to the asymmetry is relatively unaffected by any uncertainty in the values of $(1/\sigma)d\sigma/d\theta$.

## Background

Background from other than hydrogen scattering was measured by evacuating the hydrogen target and increasing the copper absorbers in *CD* and *EF* to compensate for the change in energy due to the removal of the hydrogen. The $\theta_2=15°$ background measurement immediately followed the $\theta_2=15°$ $e_{3s}$ measurement. This precaution was not taken at the other angles, since the background was significantly smaller at these larger angles.

Random backgrounds with $AB$ in random coincidence with *CD* or *EF* were also measured. Other randoms were insignificant in comparison with these. The magnitudes of the two types of background subtractions are listed in Table I.

TABLE I. Background subtractions as a percentage of the corrected counting rate.

| $\theta_2$ (deg) | Random background *ABCD* (%) | Random background *ABEF* (%) | Background *ABCD* (%) | Background *ABEF* (%) |
|---|---|---|---|---|
| 15 | 0.5 | 0.8 | 11.7 | 10.4 |
| 20 | 0.4 | 0.6 | 3.7 | 3.6 |
| 25 | 0.2 | 0.4 | 2.4 | 2.7 |
| 30 | 0.2 | 0.2 | 1.9 | 2.5 |
| 35 | 0.2 | 0.4 | 1.8 | 1.8 |
| 40 | 0.3 | 0.6 | 1.9 | 2.5 |

## $P_1P_3$

The product of incident polarization and analyzing power, $P_1P_3$, cannot be measured with the experimental arrangement used in the hydrogen scattering. The simplest method of measuring $P_1P_3$ with the available apparatus would entail the removal of the sector magnet. This would leave us with the experimental arrangement of the *R* experiment.[3] Hence, instead of repeating the measurement, an interpolation to the analyzing energies of this experiment was performed with the $P_1P_3$ results of Ref. 3.

TABLE II. $P_1(A$ experiment$)/P_1(R$ experiment$)$ versus $\theta_2$.

| $\theta_2$ (deg) | Ratio of $P_1$'s |
|---|---|
| 15 | 0.99±0.04 |
| 20 | 0.98±0.04 |
| 25 | 0.97±0.04 |
| 30 | 1.09±0.07 |
| 35 | 1.14±0.10 |
| 40 | 1.43±0.27 |

The interpolation in the analyzing energy corrected for the difference in $P_3$ between *R* and *A* experiments. It is necessary, in addition, to determine how much, if at all, $P_1$ has changed. This was done in the following fashion. With the solenoid off, the beam striking the hydrogen target will be polarized normal to the second-scattering plane, in both *R* and *A* geometries. Turning the solenoid on results in a beam which is unpolarized with respect to the normal to this second-scattering plane. Thus, by analyzing the data of the alignment profiles, which were taken for all three solenoid conditions, it is possible to obtain a measure of $P_1P_2$, where $P_2$ is the analyzing power of the hydrogen scattering. The value of $P_2$ is known as a function of energy and angle.[1] Hence, by studying the profiles from both *R* and *A* experiments, the ratio of the $P_1$ values from the two experiments could be found. In Table II the ratio $P_1(A$ experiment$)/P_1(R$ experiment$)$ is given for each scattering angle $\theta_2$. The results are based on the assumption that the polarization precesses exactly 90° in the solenoid, and indicate a ratio of 1.00 for the $P_1$ values from the two experiments. In the *R* and *A* experiments the angles of precession were, in fact, greater than 90°. When the final result is corrected for this, the ratio of the $P_1$ value for the *A* experiment to the $P_1$ value for the *R* experiment is found to be 1.01±0.04. The quoted error (all errors quoted in this paper are intended as standard deviations) is a quadratic combination of a statistical error of ±0.02 and an estimate of the systematic errors in the technique of ±0.035. The latter was inferred from systematic variations in the $P_1$ ratios listed in Table II.

The values of $P_1P_3$ used in the analysis were the interpolated values increased by the ratio of the $P_1$'s. Attached to $P_1P_3$ is a random error, which is a quadratic combination of the statistical errors on $P_1P_3$ values given in Ref. 3, and the uncertainties of the interpolation process. In addition, there is the systematic error of 4% discussed above.

## *p*-Carbon Measurement

The *A* value for proton-carbon scattering at the laboratory angle $\theta_2=15°$ was measured by the same technique as used for the *p-p* measurements. The 4-in.-diam liquid-hydrogen target was replaced by a carbon scatterer, 1.68-g/cm² thick.

There is a complication in $p$-carbon scattering not present in $p$-$p$ scattering at these energies; namely, the contribution from inelastic scattering events. The range telescopes, $CD$ and $EF$, were set to discriminate against inelastic events while still detecting elastic events with good efficiency. From the known range threshold, target thickness, and incident beam spread, one can calculate the efficiency with which the range telescopes detect scatterings with various excitation energies. This is shown in Table III.

For $p$-carbon scattering, the inelastic scattering from the 4.4- and 20-MeV levels are large. The range telescope discriminates against the latter, but not the former. The 4.4-MeV inelastic cross section has been measured at a scattering energy of 135 MeV.[7] At 15° the ratio of the 4.4 MeV inelastic cross section to the elastic cross section is 0.053. Since the efficiency for this level is 1, the inelastic contamination for scattering from the 4.4-MeV level is about 5%. The contamination from the higher levels should be much less, but no cross section measurements for these levels have been made at energies near to 138½ MeV or scattering angles near to 15°. Some measurements at[8] 182 MeV suggest the total contamination may be somewhere around 10%.

## ANALYSIS AND RESULTS

### Scattering Energy and Angle

The mean energy at the center of the hydrogen target was determined to be 139.0±1.0 MeV from range curves taken in copper at each $\theta_2$. Energy measurements are based on the polyethylene-range curves of Rich and Madey[9] and the copper range curves of Aron, Hoffman, and Williams,[10] with ranges lowered 1% to give agreement with the polyethylene curve, based on a comparison at 140 MeV. The stated error indicates the deviation of the various measurements from the mean. The energy varied with solenoid such that normal averaged higher than reverse by 1 MeV. The maximum variation was 1½ MeV. The rms deviation of the scattering energy was calculated to be ±3 MeV.

The angular resolution of the hydrogen scattering varied from ±1.5° rms at $\theta_2=15°$ to ±2.1° at $\theta_2=40°$. $\theta_2$ was determined to ±½°.

TABLE III. Telescope efficiencies for $p$-carbon scattering.

| $E$ excitation (MeV) | Efficiency |
|---|---|
| 0 (elastic) | 1 |
| 4.43 | 1 |
| 7.65 | 1 |
| 9.61 | 0.8 |
| 10.8 | 0.6 |
| 11.1 | 0.6 |
| 11.74 | 0.5 |
| 12.76 | 0.3 |
| 15.09 | 0 |

### Corrections and Errors

The measured asymmetries were corrected for random and target-empty backgrounds, and for the $\theta_3$ misalignments. The magnitudes of the backgrounds are given in Table I. The alignment correction did not exceed 0.003 in asymmetry for $\theta_2 \leq 25°$, and did not exceed 0.001 for $\theta_2 \geq 30°$. The corrected $e_{3s}$ values for $ABCD$ and $ABEF$ were averaged by weighting by the square of the reciprocal of the combined statistical and alignment errors. $A$ was calculated from $e_{3s}$ and $P_1P_3$ by Eq. (2). The above-mentioned errors on $e_{3s}$ and $P_1P_3$ were combined. The 4% systematic error in $P_1P_3$ was *not* included at this point.

A correction to the above calculated value of $A$ is necessary because of the small admixture of $R$ which was present. If the angle of bending in the sector magnet is not exactly 43.6°, there will be a transverse component present in the beam, with a corresponding mixing in of $R$ given by

$$e_{3s}=-AP_1P_3\cos\delta+RP_1P_3\sin\delta, \tag{5}$$

with $\delta=90°-\chi$. The angle of bend was measured using x-ray film to define the beam. The transverse component was also determined by moving to $\theta_2=0°$ and measuring the asymmetry. The latter measurement, designated as "$P_1P_3$," gives us $P_1P_3\sin\delta$, with $P_1P_3$ known from Ref. 3. The results of the two methods were combined, and the correction to $A$ made. This never amounted to more than 0.001 at any angle.

Because of the difference in second and third scattering energies during the background and hydrogen runs, a correction to the background is needed. The correction for $A$ was calculated only at $\theta_2=15°$ where the background was substantial. This background correction makes $A$ more positive by the amount 0.022±0.008, and is included in the final quoted value. At the other angles the change in $A$ was estimated to be of the order of one tenth of the stated error in $A$.

The previously mentioned small vertical energy variation at the slits was found to produce a change in $A$ much less than the stated uncertainties, so no corrections to $A$ were made.

The average beam energy and the monitoring efficiency change on solenoid reversal. The errors resulting from this normal-reverse difference cancel on measuring the up-down asymmetry.

One measurement of $A$ has not been included in the results. A measurement at $\theta_2=25°$ gave a value of −0.300±0.051. It would have made $A$ more positive by 0.004 or 11% of the stated total error. The current

[7] J. M. Dickson and D. C. Salter, Nuovo Cimento 6, 235 (1957).
[8] H. Tyrén and Th. A. J. Maris, Nucl. Phys. 4, 637 (1957).
[9] M. Rich and R. Madey, University of California Radiation Laboratory Report UCRL-2301, 1944 (unpublished).
[10] W. A. Aron, B. G. Hoffman, and F. C. Williams, Atomic Energy Commission Report AECU-663, 1949 (unpublished).

TABLE IV. $A$ values at 139 MeV. In addition to the errors listed (which are random and intended as standard deviations), there is a systematic error of 4% in $A$, which shifts all values up or down together.

| $\theta_2$ (deg) | $A$ |
|---|---|
| 15 | $-0.368\pm0.029$ |
| 20 | $-0.344\pm0.029$ |
| 25 | $-0.311\pm0.033$ |
| 30 | $-0.231\pm0.046$ |
| 35 | $-0.187\pm0.055$ |
| 40 | $-0.099\pm0.079$ |

regulator on the sector magnet was behaving erratically during this run.

To check on the consistency of the measurement, the $e_{3s}$ values from the $CD$ telescope were compared with those from the $EF$ telescope. Of the measurements at the six angles, three differed by less than one standard deviation, two by more than one but less than two standard deviations, and one by 2.2 standard deviations.

## Results

The final values of $A$ are listed in Table IV. The errors listed are random. Not listed is the systematic error of 4% in $A$, due to the uncertainty in $P_1$. Any analysis of these data should allow for all values shifting up or down together by, perhaps, 4%. [All errors quoted in this paper are intended as standard deviations.]

The results are also plotted in Fig. 3. The systematic error of 4% has been combined quadratically with the random error to give the error bars shown. (This combination of random and systematic error has been used in the abstract also.)

The results agree well with phase shift analyses from pre-existing data. Shown in Fig. 3 are two predictions of the Yale group,[11] YRB1 at 147 MeV and YLAM at

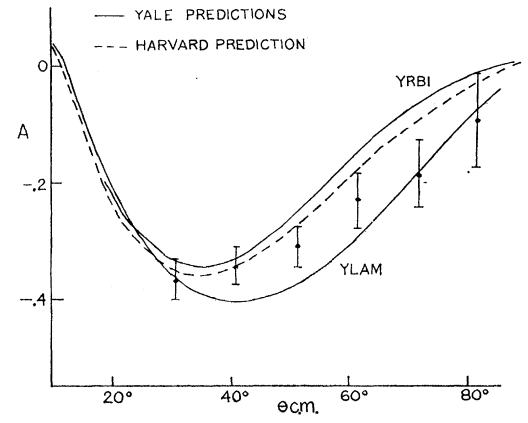


FIG. 3. A for proton-proton scattering versus center-of-mass angle $\theta_2$. Shown also are predictions of Breit *et al.* (Ref. 11) and Palmieri and Prenowitz (Ref. 12).

[11] G. Breit, M. H. Hull, K. Lassila, and K. D. Pyatt, Phys. Rev. **120**, 2227 (1960).

TABLE V. $p$-carbon results.

| Background as percentage of corrected counting rate: | | |
|---|---|---|
| | $ABCD=3.3\%$ | $ABEF=3.0\%$ |
| Energy: | $E=138\frac{1}{2}$ Mev | |
| Angle: | $\theta_2=15°$ (lab) | |
| $A$ value: | $A=-0.531\pm0.048$ | |
| Phase angle $\beta$: | $\beta=-29°\pm5°$ | |
| Predicted $R$ value: | $R=0.54\pm0.05$ | |

140 MeV. A prediction of Palmieri and Prenowitz[12] at 147 MeV is also shown. The Yale group has fitted measurements of cross section, polarization, and triple-scattering parameters over a range of energies. Measurements of $A$ at 210 MeV are included, but our measurements are not. Palmieri and Prenowitz have fitted the Harvard measurements ($\sim$140 MeV) of cross section, polarization, and triple-scattering parameters $D$ and $R$. Again, no attempt was made to fit our $A$ measurements.

Recently $A$ has been measured at 143 MeV by the Harwell group.[13] The agreement between the two sets of experimental values seems quite adequate.

## $p$-Carbon Results

The $A$ measurement for $p$-carbon scattering at $\theta_2=15°$ was similar in execution and analysis to the $p$-$p$ measurements. The energy of the second scattering was determined to be $138\frac{1}{2}$ MeV. The rms deviation of the scattering energy was $\pm3$ MeV. The angular resolution was calculated to be $\pm1.3°$.

The measured asymmetries were corrected for backgrounds, and for $\theta_3$ misalignments. The magnitudes of the backgrounds are given in Table V. The alignment correction did not exceed 0.003 in asymmetry. The correction for an admixture of $R$ made $A$ more negative by 0.002. The $A$ value obtained is $-0.531\pm0.048$.

If $\beta$ is the phase angle between $g+h$ and $g-h$, where $g$ and $h$ are, respectively, the spin-independent and spin-dependent parts of the scattering amplitude, then[4]

$$A=[1-P_2^2(\theta)]^{1/2}\sin(\beta-\theta), \tag{6}$$

where $P_2$ is the polarization produced by the carbon second scatterer, and $\theta$ is the laboratory angle of scattering. $P_2$ is a known function of energy and angle,[7,14] so Eq. (6) determines $\beta$ to within a twofold ambiguity. For $P_2=0.65\pm0.02$ we obtain values of $\beta=-29°\pm5°$ and $-121°\pm5°$. Furthermore, it is possible to derive a value of $R$ from[4]

$$R=[1-P_2^2(\theta)]^{1/2}\cos(\beta-\theta). \tag{7}$$

The values corresponding to the two values of $\beta$ above are, respectively, $R=0.54\pm0.05$ and $-0.54\pm0.05$. These are to be compared to the values $R=0.43\pm0.05$, $A=-0.49\pm0.09$, $\beta=-38°\pm3.5°$ obtained at Harwell

[12] J. N. Palmieri and E. Prenowitz (private communication).

[13] O. N. Jarvis, B. Rose, J. P. Scanlon, and E. Woods, A.E.R.E., Harwell, A.E.R.E. Report R4159 (unpublished).

[14] R. Alphonce, A. Johansson, and G. Tibell, Nucl. Phys. **4**, 672 (1957).

at 145 MeV and a lab angle of 15°.[15] We may safely conclude that the value $\beta=-29°\pm5°$ is the correct one. All the $p$-carbon results are listed in Table V. The quoted error in $A$ is a quadratic combination of the random error and the 4% systematic error mentioned in the previous section. (The $p$-carbon measurement followed immediately upon the $p$-$p$ measurements.)

[15] L. Bird, D. N. Edwards, B. Rose, A. E. Taylor, and E. Wood, J. Phys. Radium **21**, 329 (1960); B. Rose (private communication).


## ACKNOWLEDGMENTS

This experiment was a part of the nucleon-nucleon scattering program directed by Professor Richard Wilson. His support, advice, and encouragement are gratefully acknowledged. The advice and assistance of A. M. Koehler, especially in coddling a recalcitrant cyclotron, were invaluable. R. A. Hoffman generously assisted during the first run. W. Niblak participated as a Research Assistant. Miss A. Bailey, J. Holt, and L. Riseberg helped in the reduction of data.


PHYSICAL REVIEW VOLUME 132, NUMBER 2 15 OCTOBER 1963

# Neutron Photoproduction Cross Section of Calcium*

K. Min, L. N. Bolen, and W. D. Whitehead
*University of Virginia, Charlottesville, Virginia*
(Received 6 June 1963)

The photoneutron cross section of natural calcium has been measured from 15 to 30 MeV using the bremsstrahlung from the University of Virginia electron synchrotron. The neutron yields, measured in 0.5-MeV intervals, were used to unfold the photoneutron cross sections both in 1- and 0.5-MeV intervals. The cross section, which reaches the maximum value of 16.8 mb at 20.25 MeV, exhibits considerable structure. Below 21 MeV, it was possible to fit the data to the superposition of four discrete resonance curves of the Gaussian form, $\sigma=\sigma_0\exp\{-[(E_0-E)/\Delta]^2\}$, where $\sigma_0$ is the maximum cross section at energy $E_0$, and the parameter, $\Delta$, is related to the full width at half maximum, $\Gamma$, by $\Gamma=2(\ln2)^{1/2}\Delta=1.67\Delta$. The results are compared with the available shell-model calculations.

THE importance of the residual interaction between nucleons in producing the $E1$ giant resonance has been emphasized in several papers.[1–4] Detailed shell-model calculations taking into account the residual interaction have been made extensively for the closed shell nuclei. Recent measurements of[5,6] $O^{16}$ have shown that the calculated dipole-strength distribution is in good agreement with the energy positions of the structure observed in the photoneutron cross section. However, in the region of light nuclei where the $(\gamma,p)$ cross section is often comparable to, or even larger than the $(\gamma,n)$ cross section, caution is needed when one compares the partial cross-section data with the calculated absorption strengths. For the doubly magic nucleus, $Ca^{40}$, both the absorption strengths and the particle emission widths have been calculated,[7] which makes it possible to compare the results directly with the neutron cross-section measurements.

The neutron cross section of natural calcium (96.57% $Ca^{40}$) was measured using the bremsstrahlung from the University of Virginia 70-MeV electron synchrotron. A cylindrical sample of natural calcium, 3.5 cm in diameter and 14-cm long, was placed at the center of a $4\pi$ $BF_3$ paraffin-neutron detector. The neutrons emitted from the sample were detected by a system of eight $BF_3$ tubes arranged in a circle at the radial distance of 13.5 cm from the beam axis, with the total detection efficiency of 2.5%. The incident gamma-ray beam was monitored by a National Bureau of Standards type ionization chamber. The neutron yields were measured in 0.5-MeV intervals from 15 to 30 MeV of the bremsstrahlung energy. The neutron yield curve constructed from these measurements was first corrected for the background and the electronic absorption in the sample. The photoneutron cross section was unfolded from the corrected yield curve using the inverse bremsstrahlung matrix.[8]

Figure 1 shows two independent and interlacing sets

* This work was supported by the U. S. Atomic Energy Commission.

[1] J. P. Elliott and B. H. Flowers, Proc. Roy. Soc. (London) A242, 57 (1957).

[2] G. E. Brown and M. Bolstedi, Phys. Rev. Letters **3**, 472 (1959).

[3] G. E. Brown, L. Castillejo, and J. A. Evans, Nucl. Phys. **22**, 1 (1961).

[4] V. V. Balashov, V. G. Shevchenko, and N. P. Yudin, Nucl. Phys. **27**, 323 (1961).

[5] L. N. Bolen and W. D. Whitehead, Phys. Rev. Letters **9**, 458 (1962).

[6] R. L. Bramblett, J. C. Coldwell, and S. C. Fultz, University of California Lawrence Radiation Laboratory Report UCRL-7156 (unpublished).

[7] Reference 3 calculates the absorption strengths distribution. Reference 4 calculates the absorption strengths and the particle emission widths.

[8] A. S. Penfold and J. E. Leiss, Phys. Rev. **114**, 1332 (1959).